Missouri University of Science and Technology
Scholars' Mine

UMR-MEC Conference on Energy / UMR-DNR Conference on Energy

12 Oct 1978

Design and Operational Characteristics of a Retrofit Solar Heating System

D. J. Wetteroff

Bassem F. Armaly
Missouri University of Science and Technology

Follow this and additional works at: https://scholarsmine.mst.edu/umr-mec

Part of the Energy Policy Commons, Mechanical Engineering Commons, and the Power and Energy Commons

Recommended Citation

Wetteroff, D. J. and Armaly, Bassem F., "Design and Operational Characteristics of a Retrofit Solar Heating System" (1978). *UMR-MEC Conference on Energy / UMR-DNR Conference on Energy*. 388, pp. 341-347.
https://scholarsmine.mst.edu/umr-mec/388

This Article - Conference proceedings is brought to you for free and open access by Scholars' Mine. It has been accepted for inclusion in UMR-MEC Conference on Energy / UMR-DNR Conference on Energy by an authorized administrator of Scholars' Mine. This work is protected by U. S. Copyright Law. Unauthorized use including reproduction for redistribution requires the permission of the copyright holder. For more information, please contact scholarsmine@mst.edu.

DESIGN AND OPERATIONAL CHARACTERISTICS OF A RETROFIT SOLAR HEATING SYSTEM

D.J. Wetteroff and B.F. Armaly
Department of Mechanical and Aerospace Engineering
University of Missouri - Rolla
Rolla, Mo. 65401

Abstract

The construction and the operation of a retrofit solar assisted space heating system are described. Performance characteristics of each component were measured and used to estimate the contribution of solar energy to the yearly space heating energy requirements.

1. INTRODUCTION

Much of the solar heating research, development and application to date has been oriented to new housing. Retrofit of existing buildings constitutes a significant potential for solar heating application [1-3]. This type of solar application poses unique technical, economical, legal and societal problems which need to be solved before acceptable designs and construction are implemented. The literature contains little or no actual results from systems operating in the state of Missouri. This paper considers the technical aspect of this problem and reports on the design and the operation of an actual retrofit system operating on the campus of the University of Missouri Rolla. It does not deal with the optimization of system performance nor with the economic, legal or societal problems.

2. SYSTEM AND OPERATION

A small building (Bldg. T-29) on the campus of the University of Missouri-Rolla, was selected for demonstrating the feasibility of a retrofit solar space heating system. The building is a small, one story wood frame structure with 34 m^2 of floor space and a south facing pitched roof that makes a 34^o angle with the horizontal plane. The walls and the ceiling are insulated with an R-11 spun fiber glass insulation. An oil-fired furnace with forced air circulation system is used to heat the building and a window air conditioner is used for cooling.

The existing space heating system was retrofitted to utilize solar energy. The new system uses the existing oil-fired furnace as a stand-by for heating the building when the stored solar energy is not sufficient. The major components of the new system are: oil-fired furnace, solar collectors, storage unit, heat exchangers, pumps, flow loops and controls. A schematic of the flow and control diagram of the solar heating system is shown in Fig. 1. The heating system consists of three loops. The solar energy collection loop circulates anti-freeze solution through the solar collectors and then through the heat exchanger inside the water storage tank, where the energy is transferred from the anti-freeze to the water. This loop drains automatically by gravity when unfavorable conditions exist and the circulating pump stops. This circulating pump is controlled by a differential

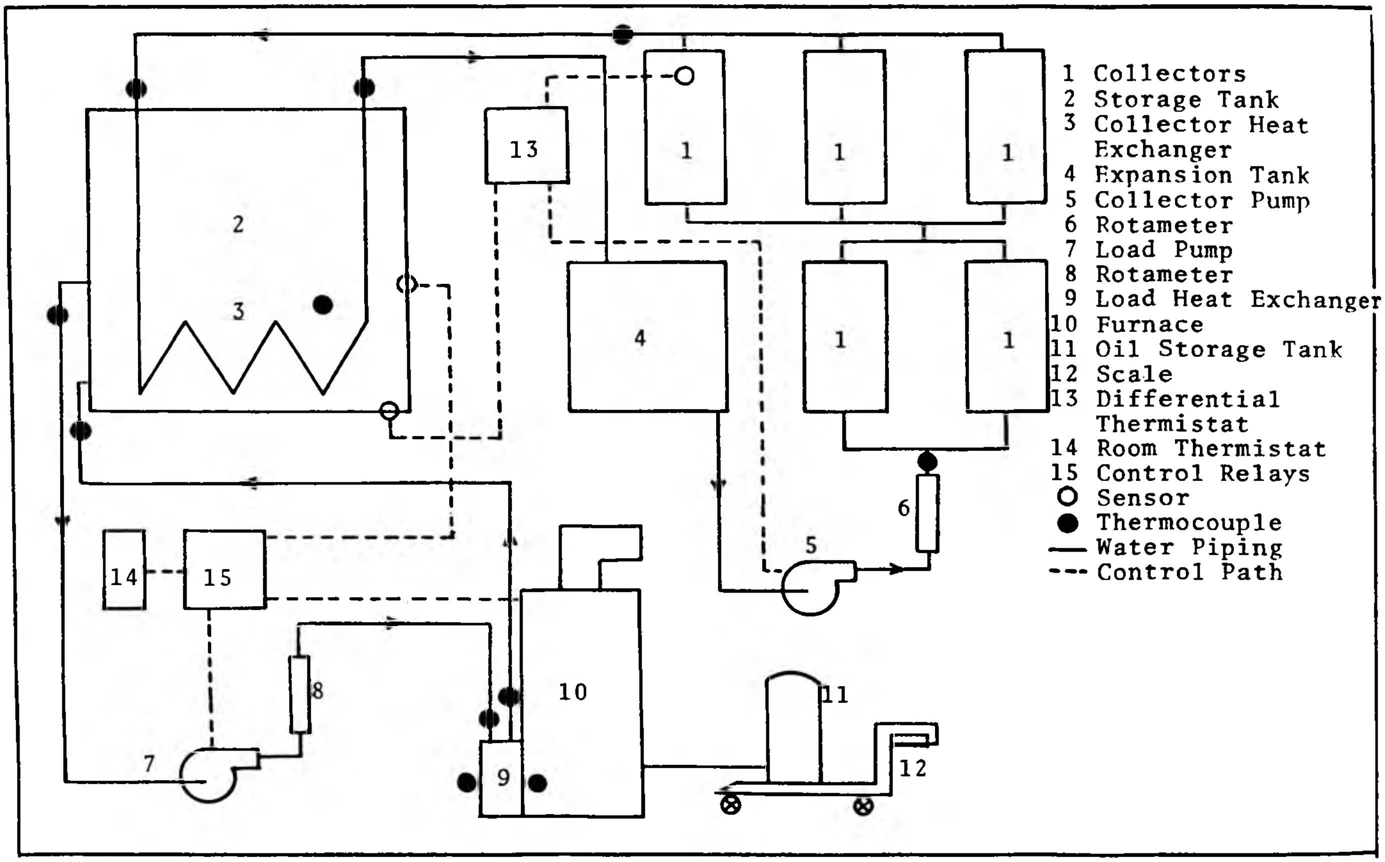

FIGURE 1 SCHEMATIC DIAGRAM OF SOLAR AND AUXILIARY HEATING SYSTEM

thermostat having one sensor attached to the collector plate and the other sensor placed in the storage tank. When the collector plate temperature is 10°C higher than the storage fluid temperature the controller activates the circulating pump. The pump operates until the collector plate temperature becomes equal to the stored fluid temperature. The heating demand loop circulates hot water from the storage tank to the load heat exchanger which is located at the inlet of the combustion chamber of the standby oil furnace. The circulation pump in this loop is controlled by a room temperature sensing thermostat, a temperature sensing element in storage tank and an assembly of control relays. When the room temperature thermostat senses a need for heat addition, the control loop has two options. Option one; if the temperature of the stored fluid is higher than 30°C the controls activate the circulating pump and the blower of the furnace without supplying fuel oil for combustion. The energy supplied to the building in this operation mode is 100% solar energy. Option two; if the temperature of the stored fluid is less than 30°C, the controls activate the normal operation of the furnace and energy supplied to the building is 100% from fuel oil. The warm air loop distributes the warm air through the building and returns it to the furnace.

Five double glazed insulated PPG Baseline collectors having a flat black, rolled bonded, aluminum absorbers are used in the solar system. The collectors are mounted flush with the roof of the building, inclined 34° to the horizontal and face due south. The total collector area is 8.36 m^2. Copper pipe is used for all the circulating loops and heat exchangers with dielectric couplings to join dissimilar metals. An insulated stainless steel water tank, volume 350 gallons, is used as a sensible heat storage unit.

3. CHARACTERISTICS OF COMPONENTS

To simulate the transient performance of the system and calculate the solar energy contribution to the space heating requirements of the building, the performance of each component in the system was measured. For example: efficiency of the solar collectors, effectiveness of the heat exchangers, overall heat transfer coefficient of the building and efficiency of the oil-fired furnace. The measurements of these parameters are described below.

Solar collectors. The solar collectors were tested in accordance with the ASHRAE testing standard 93-77 [4,5]. According to the standard the following test procedure was followed.

(1) The collectors were preconditioned by exposure to solar radiation exceeding 17,000 $KJ/(m^2\text{-day})$ for three days.

(2) The time constant for the solar collectors was determined by utilizing the following governing equation [4].

$$[F_R I_t(\tau\alpha)_e - F_R U_\ell(T_i - T_\infty) - (\dot{m}C_p/A)(T_{e,t} - T_i)]/$$
$$F_R I_t(\tau\alpha)_e - F_R U_\ell(T_i - T_\infty) - (\dot{m}C_p/A)(T_{e,i} - T_i)]$$
$$= \exp(-t/\gamma) \qquad (1)$$

where F_R is the heat removal factor, I_t is the solar insolation per unit area, $(\tau\alpha)_e$ is the effective transmittance - absorptance product of the collector cover, U_ℓ is the heat loss coefficient of the collector, T_∞ is the ambient temperature, T_i collector inlet temperature, $T_{e,i}$ collector exist temperature at time zero, $T_{e,t}$ collector exit temperature at a specified time t,γ is the time constant of the collector, $\dot{m}$ flow rate through collector, C_p specific heat and A is the frontal area of collector. The test was performed at night, I_t=0.0, and the collectors were allowed to reach steady state with an inlet fluid temperature $T_i=T_\infty+30^oC$. At that point the inlet water temperature was suddenly lowered to $T_i=T_\infty$. The transient response of the exit collector temperature to the step change in the inlet temperature is shown in Fig. 2. For the conditions described by the test (I_t=0.0, and $T_i=T_\infty$) equation (1) reduces to

$$\frac{T_{e,t} - T_i}{T_{e,i} - T_i} = \exp(-t/\gamma) \qquad (2)$$

The time constant is defined as $t=\gamma$ equivalent to the time when

$$\frac{T_{e,t} - T_i}{T_{e,i} - T_i} = 0.368 \qquad (3)$$

From Fig. 2 the time constant for the solar collectors was found to be 2.7 minutes.

(3) The near normal efficiency of the collectors was measured by operating the collector loop as an open quasi-steady state, steady flow system with constant mass flow rate and constant inlet temperature. This test was performed when the angle of the solar radiation beam was less than 30^o. Flow rates through the collectors and the difference between the inlet and outlet temperatures were measured for a quasi-steady state operating conditions. The ambient temperature and the solar radiation incident on the plane of the collectors were also measured during the test: These results were used to calculate the efficiency, η, of the collectors.

$$\eta = \frac{\dot{m}C_p(T_o - T_i)}{AI_t} \qquad (4)$$

where T_o and T_i are the exit and inlet temperature to the collector. Different operating conditions were obtained by varying the inlet fluid temperature, and the efficiency at each condition was determined. The results, which are shown in Fig. 3, were utilized with the following expression for the efficiency

$$\eta = F_R(\tau\alpha)_n - F_R U_\ell\left[\frac{(T_i - T_\infty)}{I_t}\right] \qquad (5)$$

to determine the two parameters, $F_R(\alpha\tau)_n$ and $F_R U_\ell$. The first is equivalent to the intercept of the curve with the ordinate and the second is the slope. The parameter, $(\alpha\tau)_n$ is the effective absorptance transmittance product of the collector at near normal incident.

(4) The incident angle modifier, $K(\theta)$, modifies Eq. (5) and makes it suitable for

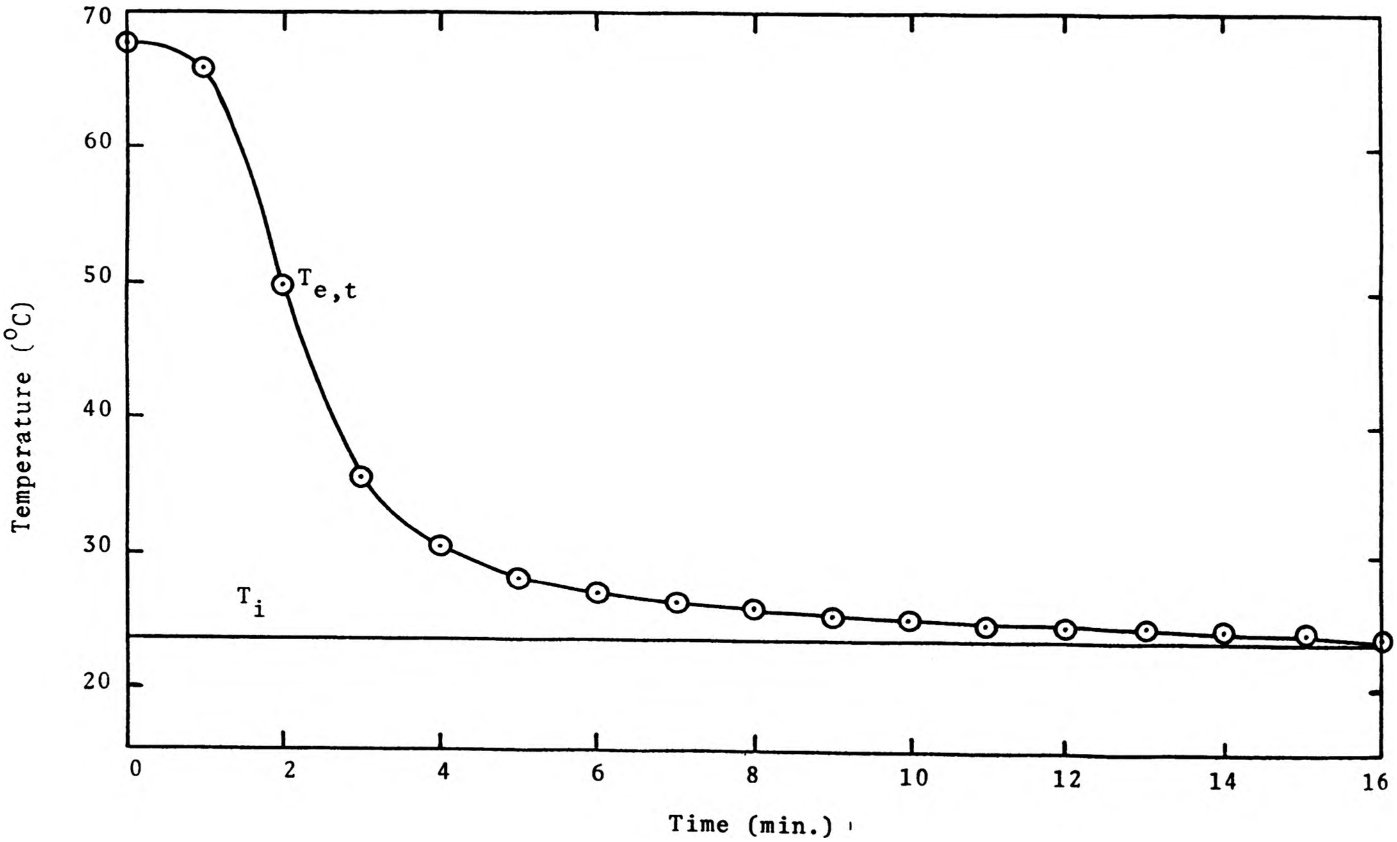

FIGURE 2 TIME CONSTANT TEST DATA

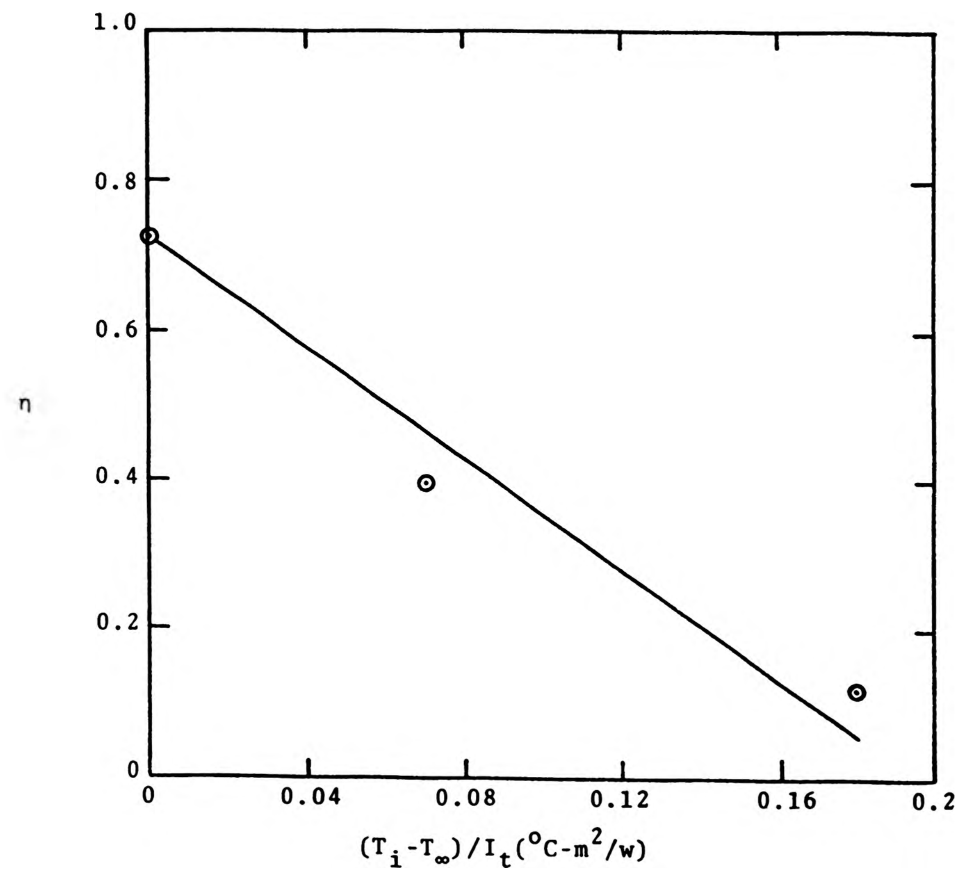

FIGURE 3 COLLECTOR EFFICIENCY

calculating the efficiency when the incident angle of the radiation beam is larger than 30°. For these conditions Eq. (5) becomes equivalent to

$$\eta = K(\theta)F_R(\tau\alpha)_n - F_RU_\ell[(T_i-T_\infty)/I_t] \qquad (6)$$

The parameter, $K(\theta)$, is determined by experimentally measuring the collector efficiency when the incident radiation angle is larger than 30°. The two parameters $F_R(\tau\alpha)_n$ and F_RU_ℓ are known from the previous tests of efficiency at near normal incident angle. The incident angle modifier which is shown in Fig. 4 can be approximated for other incident angles by utilizing the following relation.

$$K(\theta) = 1 - b_o\left(\frac{1}{\cos\theta} - 1\right) \qquad (7)$$

where b_o is the slope of the curve and θ is the incident angle.

Heat exchanger effectiveness. Two heat exchangers are used in the system. The collector heat exchanger which is located in the storage tank and the load heat exchanger which is located at the intake section of the furnace. The effectiveness of each was experimentally determined for normal operating conditions by using the following definition.

$$\varepsilon = \frac{(\dot{m}C_p)_h(T_{h,1} - T_{h,2})}{(\dot{m}C_p)_{min}(T_{h,1} - T_{C,1})} \qquad (8)$$

Where $T_{h,1}$ and $T_{h,2}$ are the inlet and exit hot fluid temperature respectively, $T_{C,1}$ is the inlet cold fluid temperature, $(\dot{m}C_p)_h$ and $(\dot{m}C_p)_{min}$ are the hot fluid and the lower capacitance fluid rate respectively. The flow rate and the temperatures at both inlets and outlets were measured for each heat exchanger. The effectiveness of the load, heat exchanger, which transfers energy from liquid to air was determined to be 0.78. The flowing air had the minimum heat capacitance rate for this situation. The effectiveness of the collector heat exchanger, which transfers energy from anti-freeze to water, was determined to be 0.70. The water in storage was stagnant and the anti-freeze flowing had the minimum heat capacitance.

Furnace Efficiency and Building Loss Coefficient. Furnace efficiency was experimentally determined by measuring the air flow rate through the furnace, the air temperatures at the inlet and outlet section and the amount of fuel oil consumed. The furnace was operating continuously and steady state conditions were reached when the above measurements were taken. The furnace efficiency was calculated to be 0.6 by using the following definition.

$$\eta_f = (\dot{m}C_p)_a(T_{a,e} - T_{a,i})/(\dot{m}_fH_f) \qquad (9)$$

Where η_f is the furnace efficiency, $(\dot{m}C_p)_a$ air capacitance rate, $\dot{m}_f$ fuel mass flow rate, H_f higher heating value of the fuel oil, and $T_{a,e}$, $T_{a,i}$ are the outlet and inlet air temperatures respectively.

The overall heat transfer coefficient of the building was determined by measuring the energy consumed to maintain the building at a specified temperature that is higher than the ambient temperature. This was determined experimentally by utilizing the oil fired furnace to maintain the inside room temperature at $18.3^{\circ}C$. This condition was controlled by the room thermostat. The ambient temperature, which was always lower than the room temperature, and the fuel oil consumed were continually recorded. This condition was maintained and monitored for one week. The data recorded were used to calculate the degree days for that period. The furnace efficiency and fuel oil consumption were used to calculate the energy input to the building. The calculated heat loss coefficient from this data was 106 Watt-hr/$^{\circ}$C-Day.

4. PREDICTIONS AND CONCLUSIONS

Data on the performance of the system over an entire heating season are not available at the present time but will be available next year. The average performance of the system was, however, predicted by using the f-chart method [6]. Reliable weather data for Rolla, Missouri are not presently available; therefore, the information for Columbia, Missouri was used (Columbia is located approximately 161 km (100 mi) northwest of Rolla). This data, which is shown in table 1, was used with the characteristics of the components in the system, which

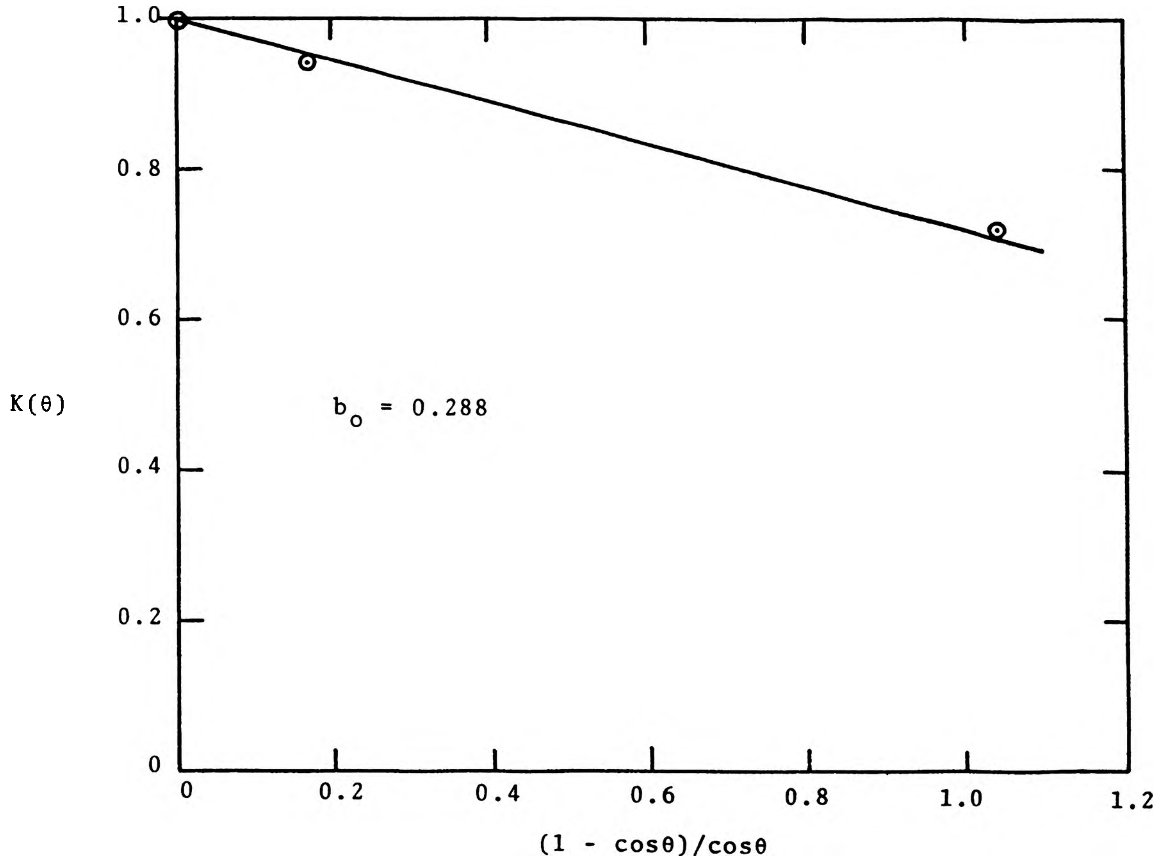

FIGURE 4 INCIDENT ANGLE MODIFIER TEST DATA

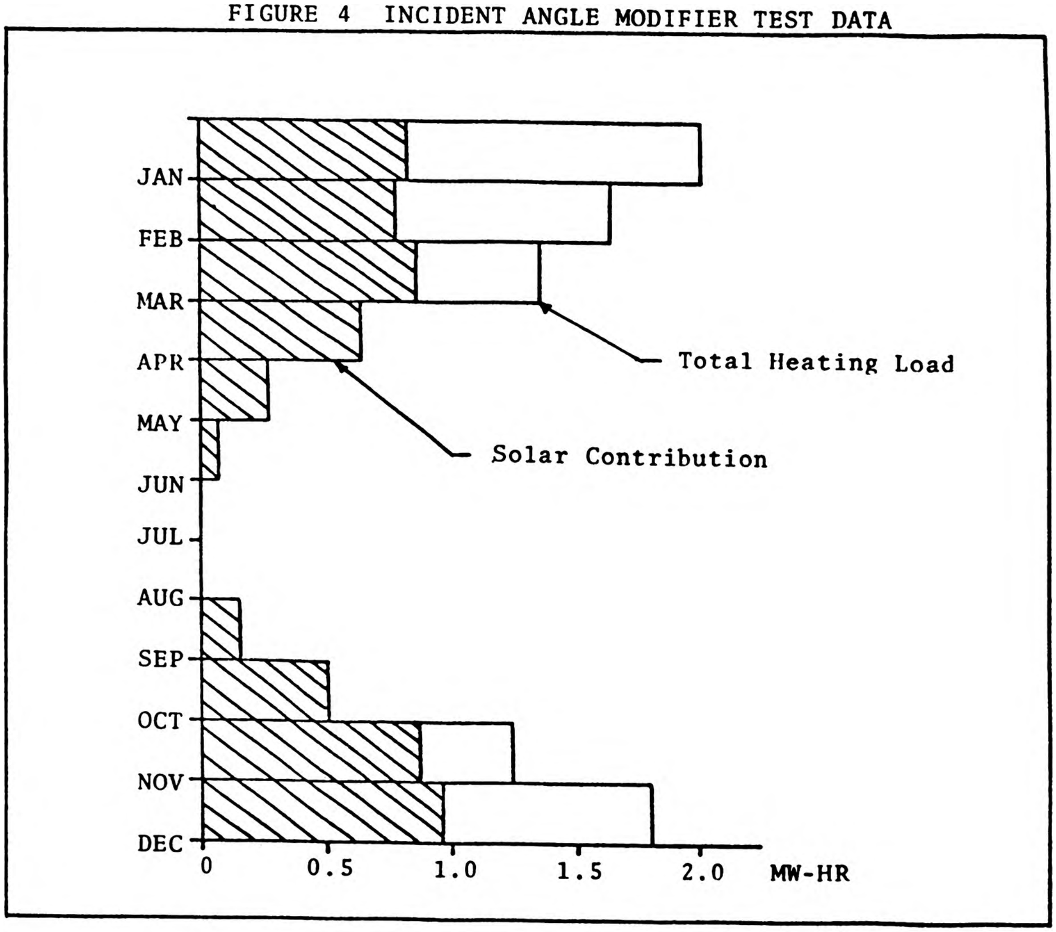

FIGURE 5 MONTHLY HEATING LOAD AND EXPECTED SOLAR CONTRIBUTION

TABLE 1
WEATHER DATA FOR COLUMBIA, MISSOURI

Month	J	F	M	A	M	J	J	A	S	O	N	D
$\bar{H}$ mJ/m^2	7.53	10.45	14.39	18.11	22.21	23.88	24.00	22.00	18.73	13.55	9.28	7.07
T_∞ °C	-1	0	6	12	18	23	25	26	20	14	6	0
°C-Day	598	486	398	180	67	7	0	0	30	139	362	537
$\bar{K}_T$	0.47	0.49	0.52	0.52	0.56	0.58	0.60	0.60	0.62	0.59	0.54	0.49

were determined in previous section, to predict the solar energy contribution to the total yearly space heating requirements of the building.

The f-chart method [6] was used to calculate the monthly fraction of heating load supplied by the solar heating system. Figure 5 compares the monthly heating load with the expected solar system performance. The annual percentage of the heating load supplied by the solar system as predicted by this method was 62%.

Measurements this winter should yield some experimental results to compare the performance of the system with the predicted performance. The heat loss coefficient of the building and the measured inside and outside temperatures will be used to calculate Degree Days and the heating load for a period of several months. The furnace efficiency and the measured consumption of fuel oil will be used to calculate the heat supplied to the building by the auxiliary system. The difference between the heating load and the heat supplied by the auxiliary system will yield the amount of heat supplied by the solar system. These results will be compared with the predicted performance.

5. REFERENCES

(1) Ragsdale, R.G. and Namkoong, O., "The NASA Langley Building Solar Project and the Supporting Lewis Solar Technology Program", NASA TM X-71600, 1971.

(2) Farber, E.A., Morrison, C.A., and Ingley, H.A., "A Case Study: Utilization of Solar Energy in Residential Dwellings", ASME 74-WA/SOL-2, 1974.

(3) Lior, N., LePore, A., and Shore, S., "Residential Solar Heating Retrofit in the Urban Environment", Joint Conference of ASISES and SES of Canada, Aug. 1976, Winnipeg, Canada.

(4) "Methods of Testing to Determine the Thermal Performance of Solar Collectors", ASHRAE Standard 93-77, ANSI B 198.1, 1977, N.Y., N.Y..

(5) Hill, J.E., "Testing of Solar Collectors According to ASHRAE Standard 93-77," ASHRAE Transactions, Vol. 84, Part II, 1978.

(6) Beckman, W.A., Klein, S.A., and Duffie, J.A., "Solar Heating Design by the f-Chart Method", John Wiley and Sons, New York, 1977.